Response to reviewer # 1

Based on CTD/XCTD obtained in May 2012 and Argo profiles along the Carlsberg Ridge, this study discussed water masses over the specific section, showed a ventilation structure, and calculated the absolute geostrophic currents. This study is interesting. However, I have the following concerns.

One of the main weaknesses is that this paper does not have a clear scientific theme and draws some quick conclusions. The authors first showed the observed temperature, salinity, and density. Then, they calculated the geostrophic currents and compared the results with SODA and HYCOM. Finally, they set some passive tracers at 100m and 700m and tried to reveal pathways of the masses. It is difficult for the readers to understand what the paper focused on, just like we cannot obtain enough information in science from the title "Hydrographic survey over the Carlsberg Ridge in May 2012" Because of no in-depth analysis, the paper looks like a data analysis report, and the conclusions are not very convinced.

I thus suggest the authors focus on the water masses in the NWIO. The authors may want to start their analysis based on the CTD/XCTD data. Then, the obtained conclusions are expected to be verified using more data (e.g. more Argo profiles) in this region and more conclusions are expected. Finally, the analysis in section 3.4 is expected to be more solid to reveal the pathway of the water masses. The authors may want to delete the contents in section 3.3.

Response: We agree with reviewer's comments and suggestions. We revised the manuscript by

(1) We added the background on meso-scale eddy and west-propagating disturbance in Introduction Section. According to Maximenko et al. (2005), the vertical structure of west-propagating disturbance has not been observed.

(2) We moved the background of Red Sea Water from Results Section into Introduction Section.

(3) We added discussions on the main results of Lagrangian tracers (Section 3.4).

Therefore the main results include the snapshot of water masses, and the vertical structures of mesoscale eddy and west-propagating disturbance.

Reference

Maximenko, N. A., Bang, B., and Sasaki, H.: Observational evidence of alternating zonal jets in the world ocean, Geophysical Research Letters, 32, L12607, 2005.

Some minor comments:

1. Could you add the latitude (or longitude) in the x-axis of Fig. 3?

Response: Corrected.

2. "Wind and SST have a close relationship." The wind pattern may be not a key factor for the SST distribution in the oceanic interior.

Response: [Page 7, line 4-6 in change-track-mode revised manuscript] We deleted the statement "Wind and SST have a close relationship".

Response to reviewer # 2

This manuscript introduces hydrographic observations collected over the Carlsberg Ridge in the northwest Indian Ocean. The authors have created a hydrographic dataset that comprises observations collected by a ship and by Argo floats. They identify key water masses, conduct particle tracking experiments, and use the observations to evaluate two re-analysis products. With a few exceptions, the standard of written English is acceptable and the quality of the figures is, on the whole, satisfactory. I think that this manuscript will require substantial revision prior to publication.
Response: We are thankful to review's encouragement and constructive suggestions. We made major revision on the early version manuscript.

Point 1. My primary criticism of this manuscript is that it lacks a clear message; I am unsure of what it is that the authors want me to remember as being important or new. The authors correctly point out that the northwest Indian Ocean is not well sampled, and so any new observations from this region are of value. However, beyond simply presenting these new observations, the authors, in my view, do not sufficiently demonstrate what we can learn from them. The discussion section, which is where the value of the new observations should be made explicit, largely restates points already made in the results section. It does not cite a single piece of literature. I think that the discussion section needs to be substantially revised: it should explain the value of the observations in the context of relevant literature and, ideally, it should set out a clear argument.
Response: The main motivation is to understand the ocean environment over Carlsberg Ridge (CR). The novelty lies on the extra information brought by in-situ CTD & XCTD data. The sectional snapshot therefore gives the vertical structures of temperature, salinity, density and geostrophic current. In the revised manuscript, we emphasized three valuable results: (1) The snapshot of water masses, (2) the structure of mesoscale eddy, and (3) the structure of west-propagating disturbance. We revised the Introduction and Discussion sections, accordingly.

Point 2. The methods outlined in section 2 need to be better explained. The authors note the depth-mean offsets between temperature and salinity observations collected by the ship's CTD and the expendable CTDs (xCTD), and between the xCTDs and an Argo float. Firstly, the implication is that these offsets used to calibrate the xCTD observations ? but this should be stated explicitly. Secondly, it is not clear to me whether: (1) xCTD observations are being compared to both ship and Argo observations; or (2) whether ship observations are being compared to xCTD observations, which are then being compared to Argo observations. If the former, which of the two sets of off- sets are the authors using for the calibration? If the latter, are the authors calibrating observations from all Argo floats using an offset calculated from just one Argo float? Furthermore, do publicly available observations from the Argo programme need to be calibrated? Are they already calibrated when they are made available for download?
Response: [Page 5, line 5 in change-track-mode revised manuscript] Good suggestions. In

section 2.1, we just clarify the differences among CTD, xCTD and Argo float. We did not calibrated the xCTD and Argo float before further low-pass filter processing. To avoid misunderstanding, we add a sentence as

”We later use objective analysis method and low-pass filter to reduce the differences among CTD, XCTD and Argo.”

Point 3. The authors point out several times that adding the Argo observations to the ship CTD and XCTD observations enables them to examine mesoscale processes. This may well be the case, but I think that they need to carefully consider the temporal and spatial scales of mesoscale activity in the Arabian Sea. For instance, they include Argo observations from up to 200 km from their section over the Carlsberg Ridge: is this distance less than the Rossby radius at this latitude? Furthermore, Table 1 indicates that the observations were collected over a period of one month. Are the authors confident that these observations may be presented in one section (Figure 4) as if they were a synoptic snapshot?

Response: In the monthly mean sea surface height (Fig. 2c in revised manuscript), two dynamics include meso-scale eddy and west-propagating disturbance are identified, we therefore confirm the two dynamics are beyond the synoptic snapshot.

Line-by-line comments.

Page 1, line 14. I am not sure what the authors mean by ”renewed” in this context.

Response: [Page 1, line 14 in change-track-mode revised manuscript] We deleted the ”renewed”.

Page 1, lines 15–17. I am not really sure what this sentence means.

Response: [Page 1, line 15-16, in change-track-mode revised manuscript]

”Moreover, the monsoon builds up a meridional current in the NWIO, which changing the form of the customary zonal current (as in the Pacific and Atlantic Oceans) into the meridional current.”

was changed to

”Moreover, the monsoon is so strong to change the pattern of basin-scale circulation. The monsoon builds up a dominant meridional current in the NWIO, which changing the form of the customary zonal current (as in the Pacific and Atlantic Oceans) into the meridional current.”

Page 1, paragraph beginning line 21. This paragraph is not relevant

Response: We deleted the paragraph.

Page 2, paragraph beginning line 13. This paragraph outlines the reasons for studying the hydrography of the Carlsberg Ridge region, but none of the points raised is revisited later in the paper. The paper would be much improved if, when discussing the results, the authors revisited some of these points for instance, saying how these new observations help to determine the movements of sporadic hydrothermal activity.

Response: [Page 13, line 21-26, in change-track-mode revised manuscript] We added the response to second reason in the Discussion Section, as

"Present paper restricts the sectional study in the upper 1050 m (Fig. 4-5). Within this depth, the water is easy affected by surface forcing. However, on the basin-scale wind-driven circulation, the surface wind forcing affects deeper ocean through quasi-geostrophic instability (Rhines and Young, 1982) and meridional overturning circulation. Generally, the hydrothermal plume in CR uplifts from sea bottom to water depth 2500 m (Murton et al., 2006; Wang et al., 2017). Because present paper concentrates on the CR as well as the cross-ridge current, the results provide potential use in the future study of hydrothermal plume event."

Page 2, line 17. I do not agree that the results presented "shed new light into the basic energy theory of ocean circulation"

Response: [Page 2, line 30, in change-track-mode revised manuscript] We weaken the statement as: "provides a reference to the basic energy theory of ocean circulation".

Page 2, line 33. It would be nice to have the distance between the CTD and the xCTD station given in km.

Response: [Page 4, line 1, in change-track-mode revised manuscript] We added the distance in km

Page 3, line 6. Again, it would be nice to have the distance between the Argo and the xCTD station given in km.

Response: [Page 4, line 6, in change-track-mode revised manuscript] We added the distance in km

Page 4, Figure 1. I think that panel (a) is too small to be of much use: I can't really see the detail because the symbols are too close together. Panel (a) might work better as a separate figure. Similarly, I cannot distinguish individual vorticity contours in panel (b). Contours are not labelled, and the contour interval is not given. The vorticity field should be presented using filled contours, similar to the ADT field in panel (d).

Response: We revised the Figure 1 according to reviewer's suggestions.

Page 5, line 28. I assume that the data extracted from the re-analysis products are along the same section as the observations, but this should be said explicitly.

Response: [Page 6, line 12, in change-track-mode revised manuscript] Yes. We added a statement in section 2.4, as

"For comparison, we extract the reanalysis datasets along the same section as the observation."

Page 6, line 8 (equations). The symbol w is not defined. I assume it is vertical velocity? The authors should state whether they are performing their particle tracking experiments using 2D or 3D velocity.

Response: [Page 6, line 18-19, in change-track-mode revised manuscript] In section 2.5, we insert two sentences, as

"w is the vertical velocity"

and
"we use the three dimensional velocity (U, V, w) to track the tracers,"

Page 6, line 10. The authors give the start and end time of the particle tracking experiments here, and not in the caption of Figure 6.
Response:[Page 6, line 20, in change-track-mode revised manuscript] Corrected.

Page 6, line 19. I do not understand what the authors mean when they say that the "wind stress curl highlights the strong seasonal variations". Also, wind stress curl is not shown in a figure.
Response: [Page 7, line 2, in change-track-mode revised manuscript] We deleted the sentence.

Page 6, line 27. The statement that warm-core eddies "seem to release footprints in the wind stress curl" does not make sense. I would have thought that the wind influences the eddies and not the other way around. Furthermore, when talking about wind stress curl, the authors refer to Figure 1 (b), but the figure caption says that this panel shows wind velocity and vorticity, not wind stress curl.
Response: [Page 7, line 10-11, in change-track-mode revised manuscript] We deleted the sentence.

Page 6, 29. It is not clear why the westward current is "remarkable". Has this feature not been observed before? Is it significant? Do the authors believe that it cannot be explained by their observations, or by existing theory?
Response: [Page 7, line 12, in change-track-mode revised manuscript] We noted the westward current "remarkable" according to the magnitude and zonal extent. As refer to Maximenko et al. (2005), present observation displays the vertical structure of this westward current. The related theory needs to be further confirmed.
Maximenko, N. A., Bang, B., and Sasaki, H.: Observational evidence of alternating zonal jets in the world ocean, Geophysical Research Letters, 32, L12607, 2005.

Page 7, line 7. Strictly speaking, the boundary between the tropics and the subtropics is around 23.5°N, so all of the observations being considered here are from the tropics. Consequently, the use of the word subtropical is misleading. Subsequent uses of these terms should also be revised.
Response: We corrected the statement accordingly. We changed the "tropical band" to "equatorial band", and changed the "subtropical band" to "tropical band" in the whole paper.

Page 7, line 7. I do not think the authors are justified in grouping PGW and RSW as RSPGIW. In Figure 2, the water masses are observed to be separate, and the authors have acknowledged the different densities of the two water masses.
Response: [Page 7, line 28-29, in change-track-mode revised manuscript] We deleted the statements related to RSPGIW.

Page 7, line 18. The observations from the World Ocean Atlas presented in Figure 3 are from a climatology and should not, therefore, be described as a snapshot.
Response: [Page 7, line 30, in change-track-mode revised manuscript] We corrected the statement.

Page 7, line 19. The authors have not marked north and south on Figure 3, so it is difficult for the reader to make sense of statements such as "the thermocline... deepens northward".
Response: [Page 18, Figure 4, in change-track-mode revised manuscript] We therefore added the latitude in Figure 3 (Figure 4 in revised manuscript).

Page 7, line 22. I do not really agree with the authors's point about ventilation. The outcropping of isotherms visible in Figure 3 is from within the mixed layer? it is not clear that "subsurface" water is then able to take part in air-sea interaction.
Response: [Page 7, line 34, in change-track-mode revised manuscript] We argue that the mixed-layer is approximately well-mixed bulk layer, which can be defined as the layer of temperature within SST minus 0.1 (or 0.5) °C. In Figure 3 (Figure 4 in revised manuscript), the interval of temperature contour is 1.0 °C, therefore, we suppose that the outcropping isothermal line was below the mixed-layer, and argue the "subsurface" water taken part in air-sea interaction.

Page 7, line 28. The authors do not explain why their observations show that saline intermediate waters are PGW and RSW ? nor do they explain why this is not clear in the climatology.
Response: [Page 10, line 5, in change-track-mode revised manuscript] Basically, we identified the PGW and RSW from T-S diagram. We added the reason in revised manuscript. For explain on the climatology, we added
"In other words, the comparison implies that the year 2002 is an anomaly year on the activities of ASHSW, PGW and RSW."

Page 7, line 31. Why have the authors chosen the 22 kg m-3 isopycnal?
Response: We chosen 22 kg m-3 because it was the first near-surface isopycnal in climatology, meanwhile, and it characterized the differences among four datasets.

Page 7, line 33. It is hard to compare Figure 1b and Figure 3, because Figure 1b uses degrees and Figure 3 uses km.
Response: [Page 18, Figure 4, in change-track-mode revised manuscript] We added the latitude in the Figure.

Page 7, line 33. I do not understand what is meant by projecting the outcrop point in the wind vector field.
Response: [Page 10, line 9, in change-track-mode revised manuscript] We deleted "when we project the outcrop point in the wind vector field".

Page 8, Figure 2. I am not sure why the mean temperature-salinity curves have been plotted. They are not mentioned in the text and they distract from the new observations.

Response: [Page 9, Figure 3, in change-track-mode revised manuscript] We moved out the mean temperature-salinity curves.

Page 9, line 1. I don't think that the thermocline can be described as descending "sharply".
Response: [Page 10, line 14, in change-track-mode revised manuscript] We changed "sharply" to "steeply".

Page 9, line 5. I don't understand what is "remarkable" about the southward extension of salty water.
Response: [Page 10, line 18, in change-track-mode revised manuscript] "the remarkable southward extension of salty water in the upper ocean"
is modified to
"the southward extension of ASHSW".

Page 9, line 15. Again, I don't understand why the velocity field in the upper ocean is "remarkable".
Response: [Page 10, line 28, in change-track-mode revised manuscript] We changed "remarkable" to "relatively strong".

Page 9, line 19. I think the authors need to label features of interest? eg CCE2 ? on Figure 4. As it stands, it is quite hard to see what the authors want the reader to look at.
Response: [Page 19 Figure 5, in change-track-mode revised manuscript] We added the position of CCE1, CCE2 and WPD in the Figure.

Page 9, line 22. The authors need to discuss, somewhere in the paper, the significance of the westward-propagating disturbance. At the end of the paper, I have no better idea of what is it and why it might be significant than I had at the start.
Response: [Page 2 line 22-24, in change-track-mode revised manuscript] In the introduction section, we added:
"The planetary waves at-least include Rossby wave, Kelvin wave and west-propagating disturbance (Rhines, 1975; McCreary, 1985). Specifically, the vertical structure of the west-propagating disturbance needs further investigation in NWIO (Maximenko et al., 2005)."

Page 9, line 26. When comparing the observationally derived geostrophic current and the current fields from the re-analysis products, have the authors considered that the current fields in the re-analysis products might contain ageostrophic components, eg Ekman flow?
Response: [Page 11 line 17-22, in change-track-mode revised manuscript] In section 3.3, we added a paragraph on discussion the Ekman flow:
"Part of the difference between observation-based absolute geostrophic current and reanalysis current is due to the near-surface Ekman current. The climatological monthly mean mixed-layer depth in May is roughly 20 m at station 9.5°N and 59.5°E (on CR; Liu et al., 2018). Besides, the mean surface Ekman speed, which is approximately the difference between surface geostrophic current and in-situ surface current (from surface drifter), is within 0.1 m/s in northern IO (Saj,

2017). Therefore, the near-surface Ekman currents in reanalysis datasets are relatively weak to affect the main results as mentioned above."

Page 10, first paragraph. I do not understand the argument that this paragraph is trying to make. There are several ideas that are not fully explored and which are insufficiently referenced. The authors seem to be contrasting "customary ventilation theory" and its corresponding meridional flow with "potential vorticity analysis" and its corresponding zonal flow. This strikes me as being a massive oversimplification; at the least, it requires a much more detailed explanation. Much of this material " as well as the extra explanation I would like to see added " probably belongs in the introduction.
Page 10, line 1. In what way are explanations of ASHSW and RSW pathways "ambiguous". This statement needs to be referenced, evidenced and more fully explained, either here or in the introduction.
Response: [Page 2 line 10-16, in change-track-mode revised manuscript] We modified the explanation, as
"For instance, three water masses were defined in NWIO as Arabian Sea High-Salinity Water (ASHSW), Persian Gulf Water (PGW) and Red Sea Water (RSW). Regarding the pathways of these water masses, the mechanics are not clear. RSW is formed near the northern side of the NWIO; therefore, according to the customary ocean ventilation theory, RSW sinks and moves southward along the isopycnal layer from the generation zone following the wind-driven current (Luyten et al., 1983). However, the feasibility of the ocean ventilation theory is still unknown for the northern IO, whose meridional extent is limited compared with the other two basins. In contrast, in situ potential vorticity analysis on RSW reveals that the flows generally follow the zonal direction (Beal et al., 2000)."
We moved the paragraph into the Introduction Section.

Page 10, line 5. This sentence is poorly expressed.
Response: [Page 2 line 14-15, in change-track-mode revised manuscript] We changed
"However, the feasibility of the ocean ventilation theory is still under debate, especially for the northern IO, whose meridional extent is limited compared with the other two basins. "
into
"However, the feasibility of the ocean ventilation theory is still unknown for the northern IO, whose meridional extent is limited compared with the other two basins."
We moved the paragraph into the Introduction Section.

Page 10, second paragraph. The authors should explain clearly why they break up the particle tracking results into latitudinal bands? is this because they suspect different processes/currents are causing differences in circulation between these bands? Also, this paragraph should make some attempt to elucidate these processes and to explain what's new and important about these results. At present, the text just explains what the reader can already see in the figure.
Page 10, line 14. I do not agree that this looks like flow in the summer Somali Current.
Response: [Page 11, line 35 – Page 12 line 15, in change-track-mode revised manuscript] We

revised the paragraph. We added:

"For better describing the trajectories, we separate the CR to three latitude bands as 2.3-5°N (equatorial band), 5-8°N and 8-9.8°N."

"In the equatorial band (Fig. 6e), the near-equator tracers come from the west side, which is consistent with the north branch of East African Coastal Current during summer monsoon (Schott and McCreary Jr., 2001; Schott et al., 2009)."

"Meanwhile, for the relatively north-side tracers in equatorial band, the trajectories backtrack to east side, which is probably following a westward current or meso-scale eddy."

"For latitudes from 8-9.8°N (Fig. 6a), the trajectories emphasis the north branch of East African Coastal Current, meanwhile, the water at the north station of CR comes from the northeast side, and one station water shows the cross-equatorial current around 53°E (east of Southern Gyre; Schott et al., 2009). "

Accordingly, we deleted:

"For the tropical band (Fig. 6e), the water mainly follows the zonal movement, but the near-equator tracers are from west side and relatively north-side tracers come from east side."

"For latitudes from 8-9.8°N (Fig. 6a), the trajectories look like the flow of the summer Somalia Current (Schott et al., 2009)"

Page 10, third paragraph. Again, some discussion of processes is needed here.

Response: [Page 12, line 16-27, in change-track-mode revised manuscript] We rewritten the paragraph. Original version:

For the RSW in the intermediate-depth layer at 700 m, the trajectories in the tropical band (Fig. 6f) and at latitudes from 5-8°N (Fig. 6d) generally follow the zonal movement (Beal et al., 2000). The tracer movements at latitudes from 8-9.8°N (Fig. 6b) partly agree with those of the ventilation theory, and partly follow the zonal direction (Beal et al., 2000).

New version:

For the RSW in the intermediate-depth layer at 700 m, the trajectories in the equatorial band (Fig. 6f) show the zonal movement. Most of the trajectories move from the west side, which coincident with the potential vorticity explanation (Beal et al, 2000), that the RSW moves southward along the coast with the help of winter monsoon, and then leave the coast and shift to middle ocean via zonal movement. Other two trajectories come from east side, and one extra trajectory moves from northwest with circular track. Hence, these trajectories display three kinds of pathways. Accordingly, in the 5-8°N band (Fig. 6d), the mainly eastward zonal movements agree with (Beal et al., 2000), meanwhile, some westward trajectories resemble the ventilation theory (Luyten et al., 1983; Qiu and Huang, 1995). At last, in the 8-9.8°N (Fig. 6b), new pathway directly from northwest is emerged, and the trajectories support 700 m waters are probably directly from east of the Horn of Africa (or Gulf of Aden) without southward movements along the coast.

Page 10, line 25. Are there papers or technical reports available that explain methodological differences between the HYCOM and SODA re-analyses? Would more thorough research negate the need for speculation?

Page 10, line 27. It is not clear to me what is meant by the "dynamic core" of the ocean general circulation model.

Response: [Page 13, line 3-14, in change-track-mode revised manuscript] We nearly rewritten the paragraph. We changed

"We speculate that although both SODA and HYCOM assimilate the Argo data into an Oceainc General Circulation Model (OGCM), the methodology of assimilation or the weight between OGCM and in situ observations, is sharply different. We assume the southward extension of ASHSW could be simulated by the dynamic core of OGCM, and the phenomenon was not captured in the Argo-only observation, therefore, HYCOM seems more to approach the dynamic model, and SODA weighted more on the Argo-only observations. Additionally, the finer horizontal resolution of HYCOM likely helps HYCOM involve more physically sound mechanics, such as the downwelling of salty water and wind-driven meridional movement."

to

"Although both SODA and HYCOM assimilate the Argo data into Oceainc General Circulation Models (OGCMs), the assimilation methods of SODA and HYCOM are considerably different. SODA adopts optimum interpolation (Carton et al., 2008), while HYCOM uses 3D variation scheme. One advantage of 3D variation scheme versus optimum interpolation is the conservation of dynamical constrains (Zhu et al., 2006; Yin et al., 2012; Edwards et al., 2015). Therefore, HYCOM probably describes better on the wind-driven circulations, monsoon-induced coastal current and meso-scale eddy movement, which are all related to the southward extension of ASHSW."

Page 10, line 33. I dislike the description of geostrophic current as an "alternative result for the ocean current". Geostrophic flow is an important part of ocean circulation and is perfectly valid in its own right.

Response: [Page 13, line 15-17, in change-track-mode revised manuscript] The sentences were deleted.

Page 11, conclusions section. The particle tracking results are not mentioned in the conclusion.

Response: [Page 14, line 14-18, in change-track-mode revised manuscript] We added paragraph in conclusion section, as

"To explore the pathways of ASHSW and RSW during the expedition time, we set tracers in SODA dataset at depths of 100 and 700 m, and backtrack their trajectories via three dimensional Lagrangian description. Overall, for the 100 m depth waters, the results reveal the pathways related to the north branch of East African Coastal Current and the flow from northeast side (or Arabian Basin), while for the 700 m depth waters, the trajectories mainly follow the zonal direction from either west and east sides. The results give direct-viewing descriptions and call for further dynamical investigations."

Page 11, line 2. The authors have not discussed baroclinic modes in the results section, so it does not make any sense to the reader when the concept is introduced in the discussion section.

Furthermore, are the authors certain that baroclinic mode is an appropriate concept in this instance?

Response: [Page 13, line 18, in change-track-mode revised manuscript] We changed the word "baroclinic" into "vertical".

Page 11, line 11. It is not correct to say that you integrate density to get the geostrophic current.

Response: [Page 14, line 1, in change-track-mode revised manuscript] We changed
"we integrate the density field to obtain the absolute geostrophic current."
into
"we compute the absolute geostrophic current based on the density profiles and sea surface height".

Page 11, line 20. I do not think that the authors have shown how "the present analysis shows potential data applications for the future".

Response: [Page 14, line 9-11, in change-track-mode revised manuscript] We changed
"The present analysis shows potential data applications for the future, where the meso-scale eddies are relatively important but cannot be well described by the Argo-only data source."
into
"Over the NWIO, the meso-scale eddies are relatively important but cannot be well described by the Argo-only data source. The present analysis shows more data source for potential data assimilation experiment."

Page 14, Figure 3. Using km as the horizontal co-ordinate is unhelpful, given that in the text what is actually interesting is the location in degrees north. The authors should also mark on features of interest discussed in the text, such as the eddies.

Response: [Page 18, Figure 4, in change-track-mode revised manuscript] We added the latitude in the Figure.

Page 16, Figure 5. Given that the westward-propagating disturbance is so little discussed, I do not think that this figure adds anything to the paper.

Response: We removed this figure.

Hydrographic survey over the Carlsberg Ridge in May 2012

Hailun He[1], Yuan Wang[2], Xiqiu Han[2], Yanzhou Wei[1], Pengfei Lin[3], Zhongyan Qiu[2], and Yejian Wang[2]

[1]State Key Laboratory of Satellite Ocean Environment Dynamics, Second Institute of Oceanography, Ministry of Natural Resources, Hangzhou 310012, China

[2]Key Laboratory of Submarine Geosciences, Second Institute of Oceanography, Ministry of Natural Resources, Hangzhou 310012, China

[3]State Key Laboratory of Numerical Modeling for Atmospheric Sciences and Geophysical Fluid Dynamics, Institute of Atmospheric Physics, Chinese Academy of Sciences, Beijing 100029, China

Correspondence: Hailun He (hehailun@sio.org.cn); Xiqiu Han (xqhan@sio.org.cn)

Abstract. In May 2012, we conducted a hydrographic survey over the Carlsberg Ridge in the northwest Indian Ocean. In this paper, we use these station data, in combination with some free-floating Argo profiles, to obtain the sectional temperature and salinity fields, and subsequently, the hydrographic characteristics are comprehensively analyzed. Through the basic T-S diagram, three salty water masses, Arabian Sea High-Salinity Water, Persian Gulf Water, and Red Sea Water, are identified. The sectional data show a clear ventilation structure associated with Arabian Sea High-Salinity Water. The 35.8 psu salty water sinks at 6.9°N and extends southward to 4.4°N at depths around the thermocline, where the thermocline depth is in the range of 100 to 150 m. This salty thermocline extends much further south than the climatology indicates. Furthermore, the temperature and salinity data are used to compute the absolute geostrophic current over the specific section, and the results show meso-scale eddy vertical structure different from some widely used oceanic reanalysis data. We also find a west-propagating disturbance at 6°N, and the related features are described in terms of phase speed, horizontal and vertical structures.

1 Introduction

The northwest Indian Ocean (NWIO) is unique compared with the other two basin-scale oceans (Pacific and Atlantic Ocean) because the dominant characteristics are monsoon driven (Schott and McCreary Jr., 2001; Schott et al., 2009). The seasonal monsoon forces the coastal current back and forth and generates the ~~renewed~~ Somalia Current, which is always marked as the strongest current in the real ocean (as strong as 3.5 m s^{-1}). Moreover, the monsoon is so strong to change the pattern of basin-scale circulation. T~~t~~he monsoon builds up a dominant meridional current in the NWIO, which changing the form of the customary zonal current (as in the Pacific and Atlantic Oceans) into the meridional current. NWIO is also famous for its role in the so-called Indian Ocean Dipole (IOD; Saji et al., 1999; Webster et al., 1999; Han et al., 2014; Chen et al., 2015), which represents the zonal gradient of sea surface temperature (SST) in the Indian Ocean (IO). As a basin-wide signal, the IOD is closely related to the IO-adjacent climate (Li and Han, 2015). Some studies also emphasized the distinct meso- and submeso-scale air-sea interactions in the NWIO (Vecchi et al., 2004).

~~Historically, the John Murray/Mabahiss expedition (1933-1934) was an early one-time IO exploration. Later, the First International Indian Ocean Expedition (IIOE-1; 1962-1965) and the subsequent Second International Indian Ocean Expedition~~

~~(IIOE-2; 2015-2020) were marked by famous international cooperation (Wooster, 1984; Aleem and Morcos, 1984; Hood et al., 2016). Between IIOE-1 and IIOE-2, the World Ocean Circulation Experiment (WOCE, 1990-1997; Ganachaud and Wunsch, 2000, 2003) defined ten one-time sections and three repeated sections in the IO (Talley, 2013). Next, considering the importance of continuous time series data, Research Moored Array for African-Asian-Australian Monsoon Analysis and Prediction (RAMA) was implemented in the tropical Indian Ocean and delivered fixed-position environmental parameters. Also, the implementation of the Array for Real-time Geostrophic Oceanography (Argo) project advanced the sampling process to be automatic and near real-time (Yin et al., 2012).~~

To date, the main water masses in the IO and NWIO are understood by the scientific community (Sharma et al., 1978; Kumar and Prasad, 1999; Emery, 2001; Talley et al., 2011)~~, although some regional water masses and their short-term variations are still not well documented~~. For instance, three water masses were defined in NWIO as Arabian Sea High-Salinity Water (ASHSW), Persian Gulf Water (PGW) and Red Sea Water (RSW). Regarding the pathways of these water masses, the mechanics are not clear. RSW is formed near the northern side of the NWIO; therefore, according to the customary ocean ventilation theory, RSW sinks and moves southward along the isopycnal layer from the generation zone following the wind-driven current (Luyten et al., 1983). However, the feasibility of the ocean ventilation theory is still unknown for the northern IO, whose meridional extent is limited compared with the other two basins. In contrast~~For instance~~, in situ potential vorticity analysis on RSW reveals that the flows generally follow the zonal direction (Beal et al., 2000).

On the other hand, the meso-scale eddies and planetary waves are not sufficiently observed in NWIO. The historical and present Research Moored Array for African-Asian-Australian Monsoon Analysis and Prediction (RAMA) ~~RAMA~~ observation arrays are close to the tropic and omit the NWIO. In situ observations in the NWIO mainly depend on Array for Real-time Geostrophic Oceanography (Argo; Riser et al., 2016; Vitale et al., 2017). However, as we show later, the number of Argo floats is still too sparse to represent the meso-scale eddy field in the NWIO. ~~The present circumstance stimulates our effort to find more observational resources.~~ The planetary waves at-least include Rossby wave, Kelvin wave and west-propagating disturbance (Rhines, 1975; McCreary, 1985). Specifically, the vertical structure of the west-propagating disturbance needs further investigation in NWIO (Maximenko et al., 2005).

The present circumstance stimulates our effort to find more observational resources. The Carlsberg Ridge (CR) is a typical slow-spreading ridge and lies along the northwest-southeast direction in the NWIO. Recently, we conducted an interdiscripline survery on CR (Yang et al., 2016; Wang et al., 2017), and the CTD and XCTD station data have not yet been explored. Hydrographic analysis of CR is necessary for at least three reasons. First, such analysis helps us to define regional ocean circulation and regional multiscale air-sea interactions. Second, the analysis supplies basic environmental parameters to determine the movements of sporadic hydrothermal activity. Third, this analysis provides a reference to ~~sheds new light into~~ the basic energy theory of ocean circulation (Huang, 1999). The trajectory of Argo float are not manually controlled; however, ship surveys could cover specified sections and have a clearer objective. Hence, this paper aims to analyze hydrographic information by combining both CR expedition and Argo floats.

2 Data and methods

2.1 In situ data description

The data for our study were collected during the Chinese cruise DY125-24 (May 2012) by the Chinese research vessel "LISIGUANG". Hydrographic observations were conducted in the region of the Carlsberg Ridge. The vertical profiles of temperature, conductivity and pressure were obtained by a calibrated SBE-19plus CTD and some expendable CTD (XCTD). The station information is shown in Fig. 1 and Table 1. All stations were mainly located along the CR section and therefore defined the regional along-section (y) and cross-section (x) coordinates. The maximum measurement depths of XCTD and Argo are 1050 and 2000 m, and therefore we limited our analysis to depth 2000 m. According to Talley et al. (2011) and Emery (2001), upper 2000 m depth covers the upper ocean (defined as 0-500 m) and the intermediate-depth ocean (defined as 500-2000 m).

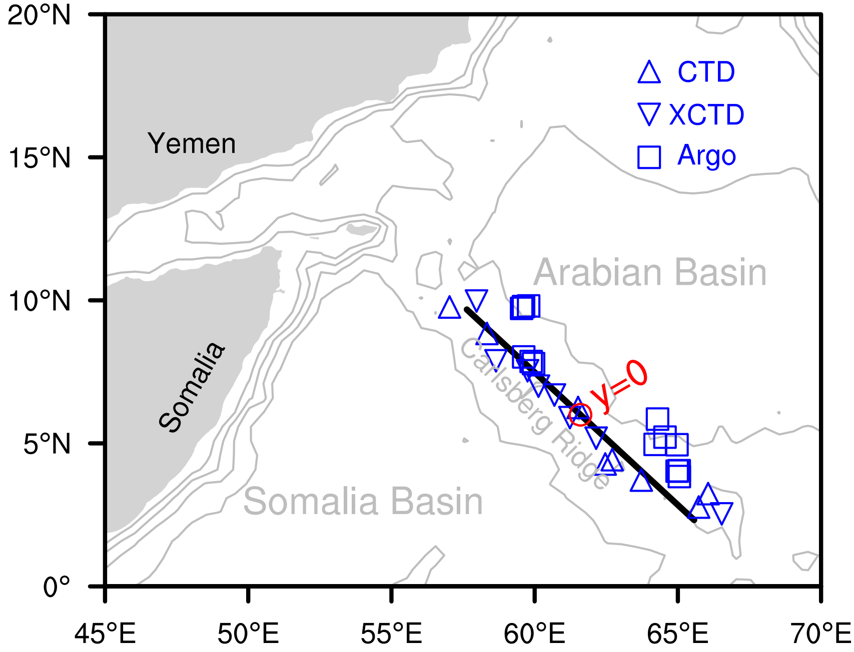

Figure 1. CTD/XCTD stations of the DY125-24 survey and the simultaneous Argo profiles around the CR. The CR defines local coordinates in which the x-coordinate is cross-track and the y-coordinate along-track, the corresponding origin point is selected as (61.6°E, 6.0°N), and the isobaths of -4000, -3000, -2000 and -1000 m are presented.

Regarding data quality, an intercomparison between XCTD and CTD measurement was implemented in the southern tropical Indian Ocean. The XCTD station involved was located at 73.8°E and 1.7°S at 14:23 on May 4 (Coordinated Universal Time), and the counterpart CTD station was located at 73.5°E and 1.4°S a half-hour later (14:58 on May 4; distance with the XCTD station as 47.17 km). The mean differences in the recorded in situ temperature (salinity) were 0.425°C (0.058 psu) in the upper ocean and 0.051°C (0.053 psu) in the intermediate-depth ocean.

Table 1. Information on CTD/XCTD stations and Argo floats.

Type	Station/Float	Latitude	Longitude	Time (month/day hour)
XCTD	S09CTD08	2.3°N	66.3°E	05/06 07
XCTD	S16CTD13	5.1°N	62.1°E	05/14 16
XCTD	S19CTD15	6.4°N	60.4°E	05/16 13
XCTD	S20CTD16	7.3°N	59.5°E	05/16 19
XCTD	S23CTD19	7.0°N	60.1°E	05/20 14
XCTD	S25CTD21	9.6°N	57.6°E	05/23 04
XCTD	S26CTD22	5.5°N	61.1°E	05/26 20
CTD	S10CTD09	3.1°N	66.0°E	05/07 05
CTD	S12CTD10	2.5°N	65.4°E	05/09 12
CTD	S14CTD11	4.2°N	62.3°E	05/11 17
CTD	S15CTD12	4.3°N	62.4°E	05/13 21
CTD	S17CTD14	6.2°N	61.3°E	05/15 08
CTD	S21CTD17	8.5°N	58.2°E	05/17 05
CTD	S22CTD18	9.5°N	57.0°E	05/18 07
CTD	S28CTD24	3.4°N	63.4°E	06/01 04
Argo	2901847	4.0°N	65.0°E	05/03 02
Argo	2901848	5.8°N	64.3°E	05/07 13
Argo	2900877	8.0°N	59.6°E	05/07 09
Argo	2901096	5.0°N	64.2°E	05/08 19
Argo	2901888	9.7°N	59.5°E	05/08 01
Argo	2901847	4.0°N	65.0°E	05/12 20
Argo	2901888	9.8°N	59.6°E	05/17 23
Argo	2900877	7.9°N	59.9°E	05/17 09
Argo	2901096	5.2°N	64.6°E	05/18 19
Argo	2901847	3.8°N	65.1°E	05/22 16
Argo	2900877	7.8°N	60.0°E	05/27 09
Argo	2901096	5.0°N	65.0°E	05/28 18
Argo	2901888	9.8°N	59.8°E	05/28 01

In our postprocessing, 13 simultaneous Argo profiles were found within a 200 km radius of the study region (Fig. 2 and Table 1). The Argo float is free-floating without regular calibration; therefore, quantifying the bias of Argo is relatively important before using the data. Fortunately, an Argo float drifted (2900877) around an XCTD station (S20CTD16; Table 1; distance with the Argo float as 79.97 km), and the two measurements occurred on May 17 and May 16, respectively. Then, we compared the XCTD with the Argo profile, and the mean differences in the in situ temperature (salinity) were 0.076°C (0.144 psu) in the upper ocean and 0.374°C (0.171 psu) in the intermediate-depth ocean. It is also noted that the differences for temperature and salinity in the intermediate depth ocean are much larger than those in the upper ocean, which is probably due to the oceanic internal high-wavenumber signals between two stations. We later use objective analysis method and low-pass filter to reduce the differences among CTD, XCTD and Argo.

2.2 In situ data processing

All the data from several sources need to be processed to same levels because of the different sampling rates; i.e., the vertical resolutions of CTD, XCTD and Argo are 0.1, 0.1, and 2.0 m, respectively. In the first step of data postprocessing, the coarse data are moving-averaged into a uniform vertical grid with a 5 m interval starting from 5 m below the surface. Here 5 m vertical resolution is sufficient for describing vertical structure of mixed-layer and water masses. Special treatment is imposed on one Argo float (2901888; three profiles; Table 1), where the coarse profiles lose data in the upper 20 m; thus, the missing data are filled with the same value as uppermost available data in the near surface.

The data are then projected into the standard CR section, with a uniform 100 km interval in the y-coordinate. We use the objective analysis method to interpolate data from irregularly spaced locations to a fixed grid (Barnes, 1994). Later, a low-pass filter is imposed on the CR sectional data to remove the short-wavelength signals, which are partly from the cross-bias among different data sources and partly from the submesoscale or higher wavenumber signals in the real ocean. The low-pass filter is a two-dimensional LOcally Estimated Scatterplot Smoothing (LOESS) filter (Cleveland and Grosse, 1991), and the moving-average wavelengths are 300 km and 30 m in the horizontal and vertical directions, respectively. As a result, the smoothed data save the essential features of the thermal-salinity field but remove the noise.

2.3 Satellite data description

2.3.1 Surface wind

We use Cross-Calibrated Multi-Platform (CCMP; Atlas et al., 2011) gridded surface vector winds here (version 2.0). CCMP data are daily products, and they are projected on 0.25°×0.25° grids.

2.3.2 Sea surface temperature

The sea surface temperature (SST) data is produced by Operational Sea Surface Temperature and Sea Ice Analysis (OSTIA; Donlon et al., 2011), which merges satellite infrared and microwave products, ship, buoy, etc. OSTIA is daily product, and the horizontal resolutions are 0.05°×0.05°.

2.3.3 Sea surface height

For describing the sea surface height (SSH) and the related surface geostrophic current, we use the Archiving, Validation, and Interpretation of Satellite Oceanographic (AVISO) grided data. The temporal resolution is daily, and the horizontal resolutions are $0.25^{\circ}\times0.25^{\circ}$.

2.4 Reanalysis data description

As references, we also employ two widely used reanalysis datasets for comparison, aiming at evaluating the quality of reanalysis data. The first reanalysis dataset is Simple Ocean Data Assimilation (SODA, version 3.3.1; Carton and Giese, 2008; Carton et al., 2018), whose horizontal resolutions are $0.25^{\circ}\times0.25^{\circ}$ for longitude and latitude. The second reanalysis dataset is HYbrid Coordinate Ocean Model (HYCOM, version GOPS3.0:HYCOM+NCODA global 1/12° Reanalysis GLBu0.08/expt_19.1), and its horizontal resolutions are $0.08^{\circ}\times0.08^{\circ}$. Both SODA and HYCOM assimilate various in situ and satellite-based data sources: historical station profiles, Argo profiles, moorings, drifters, satellite SSTs, SSHs, etc. For comparison, we extract the reanalysis datasets along the same section as the observation.

2.5 Method of tracers

Using SODA reanalysis, we release some passive tracers along the CR and backtrack their trajectories based on the Lagrangian description, and the methods are formulated by

$$\begin{cases} X^{n-1/2} & = X^{n+1/2} - U^{n}\cdot\Delta t \\ Y^{n-1/2} & = Y^{n+1/2} - V^{n}\cdot\Delta t \\ z^{n-1/2} & = z^{n+1/2} - w^{n}\cdot\Delta t \end{cases} \tag{1}$$

Here, X and Y are the Cartesian coordinates along longitude and latitude respectively, U and V are the corresponding currents, z is the vertical coordinate, w is the vertical velocity, and n is the time step. In the computation, we use the three dimensional velocity (U, V, w) to track the tracers, and we set the interval of time step (Δt) as 3600 s. The tracers are set along the CR on May 15, 2012, and then backward integrated to January 1, 2010.

3 Results

3.1 Background environment

The time period of the shipboard survey start from 2012/05/06 and end at 2012/06/01 (Table 1). Figure 2(a-c) ~~1(b-d)~~ show the monthly mean surface wind, SST and SSH, respectively. In this specific month, which is preferentially defined as the later stage of monsoon transition, the summer monsoon has started but is not very strong (Fig. 2a ~~1b~~) . The along-coast wind prevails in the regional wind field, and the wind speed in the region far from the western coast is weaker. Positive wind curl along the Somalia coast and Yemen is responsible for off-coast Ekman water transport, which induces sufficient coastal upwelling to bring lower-layer cold water upward and cool the sea surface (Fig. 2b 1c). The patterns of wind curl are roughly consistent with that of the climatological monthly mean wind stress curl (Beal et al., 2013), where the wind stress curl highlights the strong seasonal variations, particularly along the Arabian Peninsula. Otherwise, the dominant wind curl in the NWIO is negative, which is consistent with the annual mean, and denote the downwelling-preferred wind-forcing circumstance. Wind and SST have a close relationship (Fig. 1c). The near-coast Ekman pumping generates a sharp SST front at the transition area between the coast and oceanic interior. The basin-scale semicircular SST front then outlines a warm area in the oceanic interior, where SST exceeds 30°C. The main part of the CR is located in this strikingly warm region (Fig. 2b).

On the other hand, SSH (or absolute dynamic height, ADT) shows multiple meso-scale eddies (Fig. 2c 1d). There are some warm-core eddies (anti-cyclonic eddies), to the east of the CR (WCE1), east of the Horn of Africa (WCE2), and northeast of the Horn of Africa but very close to Yemen (WCE3). The first two warm-core eddies (WCE1 and WCE2) seem to release footprints in the wind stress curl (Fig.1b); however, WCE3 does not induce significant wind curl anomalies. Two cold-core eddies (cyclonic eddies; CCE1 and CCE2) are also observed at either end of the CR. Besides, a remarkable westward current is observed at the latitude of 6°N, which is noted here as a westward-propagating disturbance (WPD). WPD is pronounced compared with the circumstances around the specific region, which refers to not only the magnitude (-0.38 m/s for the zonal current) but also the zonal extent (7.5° in longitude), although its meridional extent is relatively narrow (1.3° in latitude).

3.2 Temperature, salinity and density

First, we impose the water mass analysis on the objective-analysis data (section 2.2), and the results are shown in Fig. 3. The data support that the upper water is more saline than the Indian Equatorial Water (IEW) and fresher than the Arabian Sea Water (ASW). The observed waters are likely to be mixed IEW and ASW. When the latitude spans from the equatorial tropical band (2.3-5°N in the present study) to the tropical subtropical band (5-9.7°N in the present study), the salinity generally increases, consistent with the northern-side ASW being much more saline than the southern-side IEW (Han et al., 2014) and this meridional variation in salinity is due to the different proportions of IEW and ASW. On the northwest side, water columns contain ASHSW Arabian Sea High-Salinity Water (ASHSW), which are observed as saline water at a potential density of approximately 24 kg/m^3 (Kumar and Prasad, 1999).

The intermediate waters (500 - 1500 m) from our data are projected as PGW (Prasad et al., 2001) Persian Gulf Water (PGW, Prasad et al., 2001) and RSW (Beal et al., 2000; Talley et al., 2011) Red Sea Water (RSW, Beal et al., 2000; Talley et al., 2011). According to Kumar and Prasad (1999), the definition of PGW (RSW) is the density range as 26.2-26.8 kg/m^3 (27.0-27.4 kg/m^3), temperature range 13-19°C (9-11°C), and the salinity range 35.1-37.9 psu (35.1-35.7 psu). Despite RSW is deeper than PGW, both PGW and RSW are defined as Red Sea-Persian Gulf intermediate water (RSPGIW; Emery, 2001).

Sectional profiles snapshots of temperature and salinity are shown in Fig. 4. The thermocline is in the depth range of 100 to 150 m (20°C isothermal line, Xie et al., 2002). From the present observation snapshot, the thermocline is nearly flat at the equatorial tropical band and deepens northward in the tropical subtropical band. This phenomenon is also supported by the climatological data, which reveal that the sectional distribution of the thermocline is similar to a long-standing geostrophic balanced signal. In the near surface, some isothermal lines rise to the surface on the northern side and show a clear ventila-

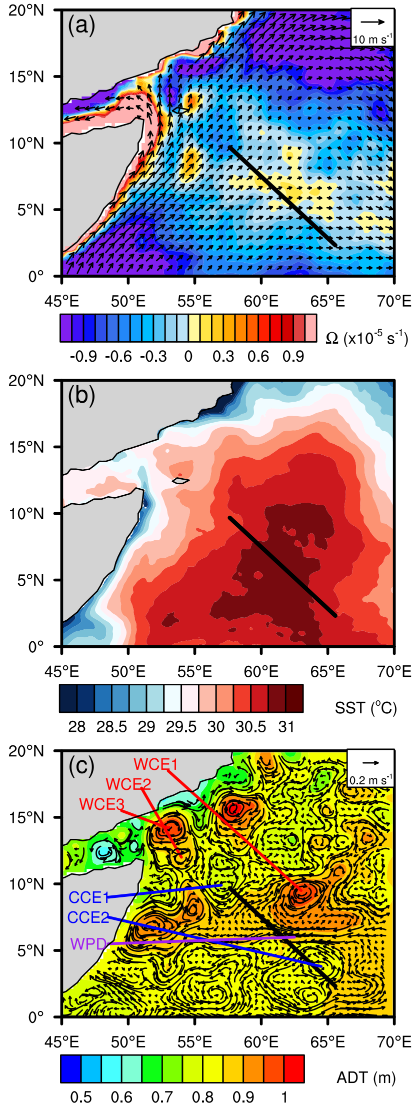

Figure 2. ~~(a) CTD/XCTD Stations of the DY24 survey and the simultaneous Argo profiles around the CR. The CR defines local coordinates in which the x-coordinate is cross-track and the y-coordinate along-track, the corresponding origin point is selected as (61.6°E, 6.0°N), and the isobaths of -4000, -3000, -2000 and -1000 m are presented;~~ (a) ~~(b)~~ monthly mean wind vector and vorticity (Ω) from CCMP wind data, data are plotted every 3 points for wind vector~~, the positive and negative vorticities are displayed by red and blue contours repectively~~; (b)~~(c)~~ monthly mean sea surface temperature from OSTIA data; and (c)~~(d)~~ monthly mean sea surface height (absolute dynamic topography), and the consistent surface geostrophic current (shown with every 2 points) from AVISO.

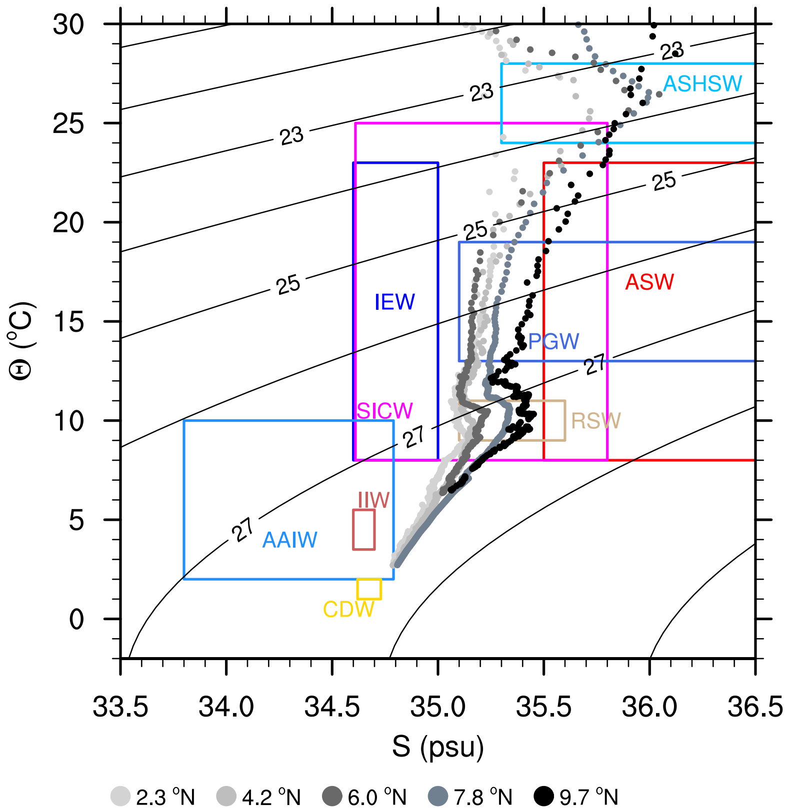

Figure 3. T-S diagram for the upper 2000 ~~1050~~ m of water on the CR. The water masses are defined in Emery (2001) and include the Arabian Sea water (ASW), Indian equatorial water (IEW), South Indian central water (SICW), Antarctic intermediate water (AAIW), Indonesian intermediate water (IIW), ~~Red Sea-Persian Gulf intermediate water (RSPGIW),~~ and circumpolar deep water (CDW). ~~The color lines are the mean T-S curves (Figure 8 in Emery (2001)), and t~~The rectangles represent the appropriate temperature and salinity ranges (Table 1 in Emery (2001)). Besides ~~In addition~~, Red Sea water (RSW), Persian Gulf water (PGW), and Arabian Sea High-Salinity Water (ASHSW) are also represented ~~in the present analysis~~ according to Kumar and Prasad (1999).

tion structure such that subsurface water can take part in the air-sea interaction. Meanwhile, for the intermediate water, the isothermal line tilts deeper from south to north.

The striking feature of the salinity field is that a salinity tongue appears at 100 m depth, where the salty water is ASHSW (Kumar and Prasad, 1999). Climatological data show that these salty waters originate from the north side and extend southward;

however, in our survey, the extent is greater. We emphasize the iso-salinity line of 35.8 psu; the southern extension can reach y=150 km (or 6.9°N) in climatology but -250 km (or 4.4°N) in our survey. This result means that the salty water extends southward more than 2.5° in latitude in excess of climatology. The present observation also shows the salty intermediate water as PGW and RSW (Fig. 3). The observation shows slightly more saline water than climatology on the northern side, although the overall structure is mostly consistent with the climatology. In other words, the comparison implies that the year 2002 is an anomaly year on the activities of ASHSW, PGW and RSW.

When we move forward to the potential density field, the appearance of the 22 kg/m^3 isopycnal is evident in both the snapshot and climatology. For the snapshot, the outcrop point of the 22 kg/m^3 isopycnal is y=300 km, or 7.8°N. It is worth noting that the outcrop point is near the transition point for signs of wind vorticity when we project the outcrop point in the wind vector field (Fig. 1b) (Fig. 2a) The north side of the outcrop point has negative wind vorticity, which promotes downwelling. Ventilation is highly related to the downwelling of high-salinity water and its southern extension (Luyten et al., 1983).

Fig. 4 also shows the reanalysis data, and essentially, the reanalysis captures the thermal structure quite well compared with the present observations and climatology. For instance, in the upper ocean, the surface warm water is distributed on the south side and northward to y=400 km where it crops out. The observed steeply sharply descending thermocline near y=100 km is reproduced in SODA and HYCOM. It is also noted that the equatorial tropical near-surface upwelling in HYCOM has some evidence from the present observations. For the intermediate-depth water, in SODA and HYCOM, the isothermal lines also tilt deeper from south to north, which resembles both the present observations and the climatology.

For salinity, the southward extension of ASHSW remarkable southward extension of salty water in the upper ocean is also captured by SODA and HYCOM, and the southward extension in HYCOM approaches the observations more closely. In the intermediate-depth water, the southward extension from the north side in SODA is similar to the observations, while the corresponding signal in HYCOM is obscured.

The upper ocean density fields from SODA and HYCOM also show clear ventilation structures. From the observations, equatorial tropical waters with a potential density of 22 kg/m^3 at a depth of 30 m are rising to the surface. The outcrop points of a potential density of 22 kg/m^3 in SODA and HYCOM are shifted southward compared with the observations. Additionally, the near-surface upwelling in the equatorial tropical band in HYCOM is strong, but not significant in the observations.

3.3 Cross-track current

The geostrophic current is deduced from the in situ density field by thermal wind theory (Fig. 5), where the velocity is integrated downward from the surface geostrophic current (Lagerloef et al., 1999). The velocity field is relatively strong remarkable in the upper ocean, where the current field is dominated by meso-scale eddies. The cross-track current in the equatorial tropical band is induced by CCE2. The structure of CCE2 is asymmetric, and the positive cross-track flow is stronger than the negative counterpart. In contrast, the northwest side of CR is identified as the south part of CCE1 (northeastward flow). In contrast, the subtropical band is identified as the margin of a warm-core eddy, which is located northwest of the CR. At 6°N latitude, the vertical structure of WPD is well rebuilt in Fig. 5a. WPD seems to extend vertically to a depth of 200 m, and the horizontal extent is near 200 km for the current greater than 0.02 m/s. Meanwhile, the maximum cross-track current of the disturbance is 0.12 m/s. Furthermore, we investigated the surface zonal current at 6°N latitude (surface geostrophic current from SSH), ~~Furthermore, Fig. 6 is the Hovmöller plot of the surface zonal current at 6°N latitude (surface geostrophic current from SSH).~~ t~~T~~he WPD are observed to start at 69°E on day 102, propagate westward with a phase speed of 0.2 m s^{-1} and arrive at 60°E on day 155 (results are not shown here). The current field also captures the northeastward ~~northeast~~ current (less than 0.075 m/s) in the intermediate depth (-200 $\leq y \leq$ -20 km, and 150 $\leq y \leq$ 350 km), which is due to the corresponding isothermal tilting (Fig. 4).

For the reanalysis data, as shown in Fig. 5, although the surface currents are similar due to the assimilation of SSH in the reanalysis process, the cross-track current from reanalysis is quite different from the observation-based absolute geostrophic current. The differences are observed in three aspects. First, the meso-scale eddy CCE2 is not well represented for the vertical structure, as SODA and HYCOM limit the southern part of CCE2 to the upper 200 m, when the current speed is faster than 0.05 m/s. Meanwhile, in SODA and HYCOM, the northern part of the meso-scale eddy (CCE2) has much latitude expansion, and merges the disturbance (WPD). Second, the undercurrent in the southern portion of the observations differs from those in SODA and HYCOM. The undercurrent in SODA is relatively weak, while HYCOM shows a northward shift of the current core. Finally, for the northern portion, SODA gives a relatively shallow depth for the surface northeastward ~~northeast~~ current, and the corresponding horizontal extent exceeds that of the observations. The locations of surface zero current in SODA and observation are y=170 and 240 km, respectively.

Part of the difference between observation-based absolute geostrophic current and reanalysis current is due to the near-surface Ekman current. The climatological monthly mean mixed-layer depth in May is roughly 20 m at station 9.5°N and 59.5°E (on CR; Liu et al., 2018). Besides, the mean surface Ekman speed, which is approximately the difference between surface geostrophic current and in-situ surface current (from surface drifter), is within 0.1 m/s in northern IO (Saj, 2017). Therefore, the near-surface Ekman currents in reanalysis datasets are relatively weak to affect the main results as mentioned above.

3.4 Tracers

~~Where the pathways of ASHSW and RSW are concerned, the explanations are still ambiguous. ASHSW and RSW are formed near the northern side of the NWIO; therefore, according to the customary ocean ventilation theory, ASHSW and RSW sink and move southward along the isopycnal layer from the generation zone following the wind-driven current (Luyten et al., 1983). However, in the northern IO, the meridional extent is limited as compared with the other two basins, whether the the ocean ventilation theory is feasible in northern IO is under debate. However, the feasibility of the ocean ventilation theory is still under debate, especially for the northern IO, whose meridional extent is limited compared with the other two basins. For instance, in situ potential vorticity analysis on RSW reveals that the flows generally follow the zonal direction (Beal et al., 2000).~~

Here, the SODA reanalysis supplies compact datasets for passive tracers; therefore, we set some passive tracers along the CR and backtrack their trajectories using the Lagrangian description (section 2.5), and the results are shown in Fig. 6. For the ASHSW, we set the tracers at a depth of 100 m, and the trajectories reveal different pathways on the CR. For better describing the trajectories, we separate the CR to three latitude bands as 2.3-5°N (equatorial band), 5-8°N and 8-9.8°N. For the tropical band (Fig. 6e), the water mainly follows the zonal movement, but the near-equator tracers are from west side and relatively north-side tracers come from east side. In the equatorial band (Fig. 6e), the near-equator tracers come from the west side, which is consistent with the north branch of East African Coastal Current during summer monsoon (Schott and McCreary Jr., 2001; Schott et al., 2009). Meanwhile, for the relatively north-side tracers in equatorial band, the trajectories backtrack to east side, which is probably following a westward current or meso-scale eddy. While for latitudes from 5-8°N (Fig. 6c), the water mainly originates from the northeast side, and the trajectories resemble those of the ventilation theory (Luyten et al., 1983; Qiu and Huang, 1995). The results support ASHSWs are mainly from the Arabian Basin, which agrees with the ASHSW definition, and the southwestward flow bring the ASHSW into CR. In some occasions, the 100 m depth waters in this latitude section are from the equator, and the pathways show the north branch of East African Coastal Current and the cross-equatorial current around 66°E respectively. Similarly, the pathways start at the east of the Horn of Africa are probably due to the off-coast current at the north of Great Whirl or meso-scale eddies (Chelton et al., 2011; Wang et al., 2019). For latitudes from 8-9.8°N (Fig. 6a), the trajectories look like the flow of the summer Somalia Current (Schott et al., 2009). the trajectories emphasis the north branch of East African Coastal Current, meanwhile, the water at the north station of CR comes from the northeast side, and one station water shows the cross-equatorial current around 53°E (east of Southern Gyre; Schott et al., 2009).

For the RSW in the intermediate-depth layer at 700 m, the trajectories in the tropical band (Fig. 6f) and at latitudes from 5-8°N (Fig. 6d) generally follow the zonal movement (Beal et al., 2000). The tracer movements at latitudes from 8-9.8°N (Fig. 6b) partly agree with those of the ventilation theory, and partly follow the zonal direction (Beal et al., 2000).

For the RSW in the intermediate-depth layer at 700 m, the trajectories in the equatorial band (Fig. 6f) show the zonal movement. Most of the trajectories move from the west side, which coincident with the potential vorticity explanation (Beal et al., 2000), that the RSW moves southward along the coast with the help of winter monsoon, and then leave the coast and shift to middle ocean via zonal movement. Other two trajectories come from east side, and one extra trajectory moves from northwest with circular track. Hence, these trajectories display three kinds of pathways. Accordingly, in the 5-8°N band (Fig. 6d), the mainly eastward zonal movements agree with Beal et al. (2000), meanwhile, some westward trajectories resemble the ventilation theory (Luyten et al., 1983; Qiu and Huang, 1995). At last, in the 8-9.8°N (Fig. 6b), new pathway directly from northwest is emerged, and the trajectories support 700 m waters are probably directly from east of the Horn of Africa (or Gulf of Aden) without southward movements along the coast.

4 Discussion

The CTD and XCTD data are precise in reconstructing the three-dimensional oceanic data. The Argo-only data are not sufficient to describe the meso-scale eddy in the NWIO. In the present study, the maximum distance between Argo profiles is 500 km along the CR; however, after adding the shipboard station data, the maximum distance decreases to 100 km, which falls into the eddy-permitting scale. Sufficient sampling produces more reliable vertical structures of temperature, salinity and density.

The most remarkable signal in the upper ocean is the southward extension of ASHSW, where the counterpart in the climatology data exists but is weak in the horizontal extension. It is surprising that the HYCOM reanalysis captures the phenomenon well, while SODA shows some disadvantages. Although both SODA and HYCOM assimilate the Argo data into Oceainc General Circulation Models (OGCMs), the assimilation methods of SODA and HYCOM are considerably different. SODA adopts optimum interpolation (Carton et al., 2018), while HYCOM uses 3D variation scheme. One advantage of 3D variation scheme versus optimum interpolation is the conservation of dynamical constrains (Zhu et al., 2006; Yin et al., 2012; Edwards et al., 2015). Therefore, HYCOM probably describes better on the wind-driven circulations, monsoon-induced coastal current and meso-scale eddy movement, which are all related to the southward extension of ASHSW. We speculate that although both SODA and HYCOM assimilate the Argo data into an Oceainc General Circulation Model (OGCM), the methodology of assimilation or the weight between OGCM and in situ observations, is sharply different. We assume the southward extension of ASHSW could be simulated by the dynamic core of OGCM, and the phenomenon was not captured in the Argo-only observation, therefore, HYCOM seems more to approach the dynamic model, and SODA weighted more on the Argo-only observations. Additionally, the finer horizontal resolution of HYCOM likely helps HYCOM involve more physically sound mechanics, such as the downwelling of salty water and wind-driven meridional movement.

Although the geostrophic balance is not universally suitable, it represents a good approximation to the real ocean; therefore, under the circumstance without in situ current observations, the deduced absolute geostrophic current gives alternative results for the ocean current. In the comparative analysis, the state-of-the-art reanalysis is still insufficient to provide good current data. Although similar sea surface dynamic heights are taken into account, the incorrect density field leads to a false vertical baroclinic mode. It is also noted that the bias is probably further amplified in OGCM and leads to potential unrealistic simulations if these reanalysis data are used in the model for initialization and boundary forcing.

Present paper restricts the sectional study in the upper 1050 m (Fig. 4-5). Within this depth, the water is easy affected by surface forcing. However, on the basin-scale wind-driven circulation, the surface wind forcing affects deeper ocean through quasi-geostrophic instability (Rhines and Young, 1982) and meridional overturning circulation. Generally, the hydrothermal plume in CR uplifts from sea bottom to water depth 2500 m (Murton et al., 2006; Wang et al., 2017). Because present paper concentrates on the CR as well as the cross-ridge current, the results provide potential use in the future study of hydrothermal plume event.

5 Conclusions

This paper reports a onetime hydrographic survey on the CR in the NWIO, where the latitudes cover the equatorial tropical (2.3-5°N) and tropical subtropical (5-9.6°N) bands. The station CTD/XCTD sampling plus the Argo floats build the sectional structures of temperature and salinity as well as density. The striking feature is the southern extension of ASHSW from northwest of the CR in the upper ocean. Meanwhile, the temperature and density fields display clear ventilation structures. In the intermediate depth, the observations also capture the RSW at a depth near 700 m.

Furthermore, we compute the absolute geostrophic current based on the density profiles and sea surface height ~~we integrate the density field to obtain the absolute geostrophic current~~. The vertical structure of the cross-track current reveals strong signals of meso-scale eddies in the upper ocean and relatively weak northeastward current in the intermediate depth. We also identify a strong westward-propagating disturbance at a latitude of 6°N. The longitude and latitude lengths are 7.5° and 1.3° respectively. The corresponding phase speed is 0.2 m/s, and the vertically affected depth is roughly 200 m.

We further evaluate the state-of-the-art reanalysis with the present observations. As a result, because the Argo profiles and satellite SSH are assimilated into the reanalysis datasets, HYCOM and SODA show relatively good qualities for temperature, salinity and density. However, the reanalysis cross-track currents show large discrepancies compared with the absolute geostrophic current. Most importantly, HYCOM and SODA misinterpret some meso-scale eddies in the current field. Over the NWIO, the meso-scale eddies are relatively important but cannot be well described by the Argo-only data source. The present analysis shows more data source for potential data assimilation experiment. ~~The present analysis shows potential data applications for the future, where the meso-scale eddies are relatively important but cannot be well described by the Argo-only data source.~~ The present situation of insufficient sampling prompts more research activity in the NWIO.

To explore the pathways of ASHSW and RSW during the expedition time, we set tracers in SODA dataset at depths of 100 and 700 m, and backtrack their trajectories via three dimensional Lagrangian description. Overall, for the 100 m depth waters, the results reveal the pathways related to the north branch of East African Coastal Current and the flow from northeast side (or Arabian Basin), while for the 700 m depth waters, the trajectories mainly follow the zonal direction from either west and east sides. The results give direct-viewing descriptions and call for further dynamical investigations.

Competing interests. The authors declare that they have no conflict of interest.

Acknowledgements. This work is supported by the China Ocean Mineral Resources Research and Development Association Project (Nos. DY135-S2-1-07 and DY135-E2-1-01) and the National Natural Science Foundation of China (Nos. 41730535 and 41621064). OSTIA SST data were produced by the Meteorological Office of the United Kingdom (http://marine.copernicus.eu/). We are thankful to two anonymous reviewers for their constructive suggestions and comments. WOA data were available in https://www.nodc.noaa.gov/. Daily Argo float data were downloaded from http://www.argodatamgt.org. CCMP wind were provided by Remote Sensing Systems (http://www.remss.com, version 2.0), AVISO SSH data were produced and distributed by the Copernicus Marine and Environment Monitoring Service (CMEMS) (http://www.marine.copernicus.eu), SODA were obtained from http://www.atmos.umd.edu/ ocean/, and HYCOM were downloaded from https://hycom.org/.

References

Atlas, R., Hoffman, R. N., Ardizzone, J., Leidner, S. M., Jusem, J. C., Smith, D. K., and Gombos, D.: A cross-calibrated, multiplatform ocean surface wind velocity product for meteorological and oceanographic applications, Bull. Amer. Meteor. Soc., 92, 157–174, 2011.

Barnes, S. L.: Applications of the Barnes Objective Analysis Scheme. Part I: Effects of Undersampling, Wave Position, and Station Randomness, J. Atmos. Oceanic Technol., 11, 1433–1448, 1994.

Beal, L. M., Ffield, A., and Gordon, A. L.: Spreading of Rea Sea overflow waters in the Indian Ocean, J. Geophys. Res., 105, 8549–8564, 2000.

Beal, L. M., Hormann, V., Lumpkin, R., and Foltz, G.: The Response of the Surface Circulation of the Arabian Sea to Monsoonal Forcing, J. Phys. Oceanogr., 43, 2008–2022, 2013.

Carton, J. A. and Giese, B. S.: A reanalysis of ocean climate using Simple Ocean Data Assimilation (SODA), Monthly Weather Review, 136, 2999–3017, 2008.

Carton, J. A., Chepurin, G. A., and Chen, L. G.: SODA3: A new ocean climate reanalysis, J. Clim., 31, 6967–6983, 2018.

Chelton, D. B., Schlax, M. G., and M., S. R.: Global observations of nonlinear mesoscale eddies, Progress in Oceanography, 91, 167–216, 2011.

Chen, G. X., Han, W. Q., Li, Y. L., Wang, D. X., and J., M. M.: Seasonal-to-interannual time scale dynamics of the equatorial undercurrent in the Indian Ocean, J. Phys. Oceanogr., 54, 1532–1553, 2015.

Cleveland, W. S. and Grosse, E.: Computational methods for local regression, Stat. Comput., 1, 47–62, 1991.

Donlon, C. J., Martin, M., Stark, J. D., Roberts-Jones, J., E., F., and W., W.: The Operational Sea Surface Temperature and Sea Ice analysis (OSTIA), Remote Sensing of the Environment, 116, 140–158, 2011.

Edwards, C. A., Moore, A. M., Hoteit, I., and Cornuelle, B. D.: Regional ocean data assimilation, Annual Review of Marine Science, 7, 21–42, 2015.

Emery, W. J.: Water Types and Water Masses*, in: Encyclopedia of Ocean Sciences (Second Edition), edited by Steele, J. H., pp. 291 – 299, Academic Press, Oxford, second edition edn., https://doi.org/https://doi.org/10.1016/B978-012374473-9.00108-9, 2001.

Han, W. Q., Vialard, J., McPhaden, M. J., Lee, T., Masumoto, Y., Feng, M., and DE Ruijter, W. P. M.: Indian Ocean decadal variability: A review, Bulletin of the American Meteorological Society, 95, 1679–1703, 2014.

Huang, R. X.: Mixing and energetics of the oceanic thermohaline circulation, J. Phys. Oceanogr., 29, 727–746, 1999.

Kumar, S. P. and Prasad, T. G.: Formation and spreading of Arabian Sea high-salinity water mass, J. Geophys. Res. Oceans, 104, 1455–1464, 1999.

Lagerloef, G. S. E., Mitchum, G. T., Lukas, R. B., and Niiler, P. P.: Tropical Pacific near-surface currents estimated from altimeter, wind, and drifter data, J. Geophys. Res.-Oceans, 104, 23 313–23 326, 1999.

Li, Y. L. and Han, W. Q.: Decadal sea level variations in the Indian Ocean investigated with HYCOM: Roles of climate modes, ocean internal variability, and stochastic wind forcing, J. Clim., 28, 9143–9165, 2015.

Liu, L. L., Huang, R. X., and Wang, F.: Ventilation of a monsoon-dominated ocean: Subduction and obduction in the North Indian Ocean, J. Geophys. Res. Oceans, 123, 4449–4463, 2018.

Luyten, J. L., Pedlosky, J., and Stommel, H. M.: The ventilated thermocline, J. Phys. Oceanogr., 13, 292–309, 1983.

Maximenko, N. A., Bang, B., and Sasaki, H.: Observational evidence of alternating zonal jets in the world ocean, Geophysical Research Letters, 32, L12607, https://doi.org/10.1029/2005GL022728, 2005.

McCreary, J. P.: Modeling equatorial ocean circulation, Annual Review of Fluid Mechanics, 17, 359–409, 1985.

Murton, B. J., Baker, W. T., Sands, C. M., and German, C. R.: Detection of an unusually large hydrothermal event plume above the slow-spreading Carlsberg Ridge: NW Indian Ocean, Geophys. Res. Lett., 33, L10608, 2006.

Prasad, T. G., Ikeda, M., and Kumar, S. P.: Seasonal spreading of the Persian Gulf Water mass in the Arabian Sea, J. Geophys. Res. Oceans, 106, 17 059–17 071, 2001.

Qiu, B. and Huang, R. X.: Ventilation of the North Atlantic and North Pacific: Subduction versus obduction, J. Phys. Oceanogr., 25, 2374–2390, 1995.

Rhines, P. B.: Waves and turbulence on a beta-plane, J. Fluid Mech., 69, 417–443, 1975.

Rhines, P. B. and Young, W. R.: Homogenization of potential vorticity in planetary gyres, J. Fluid Mech., 122, 347–367, 1982.

Riser, S. C., Freeland, H. J., Roemmich, D., Wijffels, S., Troisi, A., Belbeoch, M., Gilbert, D., Xu, J., Pouliquen, S., Thresher, A., Le Traon, P.-Y., Maze, G., Klein, B., Ravichandran, M., Grant, F., Poulain, P.-M., Suga, T., Lim, B., Sterl, A., Sutton, P., Mork, K.-A., Velez-Belchi, P. J., Ansorge, I., King, B., Turton, J., Baringer, M., and Jayne, S. R.: Fifteen years of ocean observations with the global Argo array, Nature Climate Change, 6, 145–153, 2016.

Saj, R. P.: Surface velocity estimates of the North Indian Ocean from satellite gravity and altimeter missions, International Journal of Remote Sensing, 38, 296–313, 2017.

Saji, N. H., Goswami, B. N., Vinayachandran, P. N., and Yamagata, T.: A dipole mode in the tropical Indian Ocean, Nature, 401, 360–363, 1999.

Schott, F. A. and McCreary Jr., J. P.: The monsoon circulation of the Indian Ocean, Progress in Oceanography, 51, 1–123, 2001.

Schott, F. A., Xie, S. P., and McCreary Jr., J. P.: Indian Ocean circulation and climate variability, Reviews of Geophysics, 47, RG1002, 2009.

Sharma, G. S., Gouveia, A. D., and Satyendranath, S.: Incursion of the Pacific Ocean water into the Indian Ocean, Proc. Indian Acad. Sci., 87A, 29–45, 1978.

Talley, L. D., Pickard, G. L., Emery, W. J., and S., J. H.: Descriptive physical oceanography: An introduction, Elsevier, Burlingham, 6 edn., 2011.

Vecchi, G. A., Xie, S. P., and Fischer, A. S.: Ocean-atmosphere covariability in the Western Arabian Sea, Journal of Climate, 17, 1213–1224, 2004.

Vitale, S. S., DiMarco, S. F., Seidel, H. F., and Wang, Z. K.: Circulation analysis in the northwest Indian Ocean using ARGO floats and surface drifter observations, and SODA reanalysis output, Dynamics of Atmospheres and Oceans, 78, 57–70, 2017.

Wang, S., Zhu, W. J., Ma, J., Ji, J. L., Yang, J. S., and Dong, C. M.: Variability of the Great Whirl and its impacts on atmospheric processes, Remote Sensing, 11, 322, 2019.

Wang, Y. J., Han, X. Q., Petersen, S., Frische, M., Qiu, Z. Y., Li, H. M., Li, H. L., Wu, Z. C., and Cui, R. Y.: Mineralogy and trace element geochemistry of sulfide minerals from the Wocan Hydrothermal Field on the slow-spreading Carlsberg Ridge Indian Ocean, Ore Geology Reviews, 84, 1–19, 2017.

Webster, P. J., Moore, A. M., Loschnigg, J. P., and Leben, R. R.: Coupled ocean-atmosphere dynamics in the Indian Ocean during 1997-98, Nature, 401, 356–360, 1999.

Xie, S. P., Annamalai, H., Schott, F. A., and McCreary Jr., J. P.: Structure and mechanisms of south Indian Ocean climate variability, J Clim, 15, 864–878, 2002.

Yang, G., He, H. L., Wang, Y., Han, X. Q., and Wang, Y. J.: Evaluating a satellite-based sea surface temperature by shipboard survey in the Northwest Indian Ocean, Acta Oceanologica Sinica, 35, 52–58, 2016.

Yin, X. Q., Qiao, F. L., Yang, Y. Z., Xia, C. S., and Chen, X. Y.: Argo data assimilation in ocean general circulation model of Northwest Pacific Ocean, Ocean Dynamics, 62, 1059–1071, 2012.

Zhu, J., Zhou, G. Q., X., Y. C., Fu, W. W., and You, X. B.: A three-dimensional variational ocean data assimilation system: Scheme and preliminary results, Science in China Series D: Earth Sciences, 49, 1212–1222, 2006.

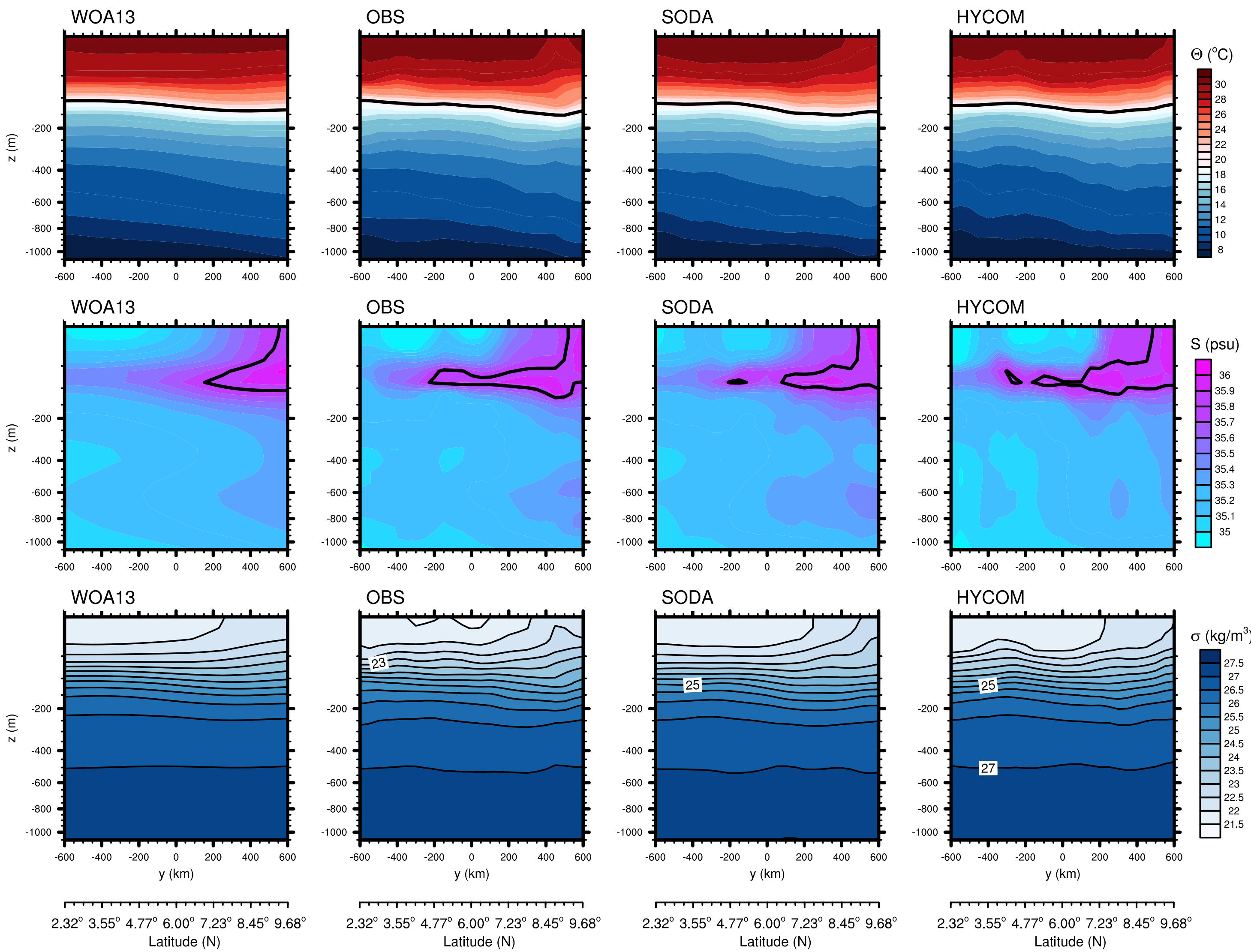

Figure 4. Sectional profiles of potential temperature (upper panels), salinity (middle panels) and potential density (lower panels). The data sources cover the WOA climatology (WOA13, version 2.0/A5B2), the present observations, and two reanalysis datasets, SODA and HYCOM. The isothermal lines of 20°C are presented at potential temperatures, and the iso-salinity lines of 35.8 psu are highlighted in the salinity fields.

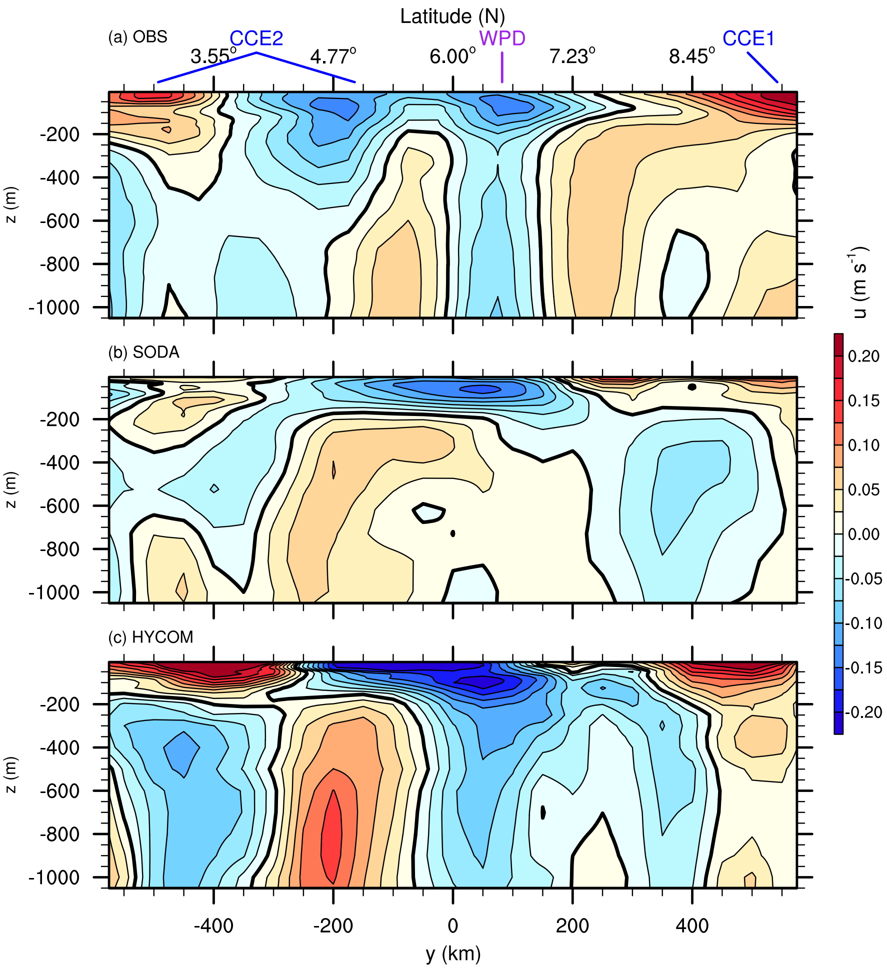

Figure 5. Sectional cross-track current: (a) absolute geostrophic current; (b and c) currents in SODA and HYCOM reanalysis, respectively. Northeastward current is positive. Thick black lines are the zero contours.

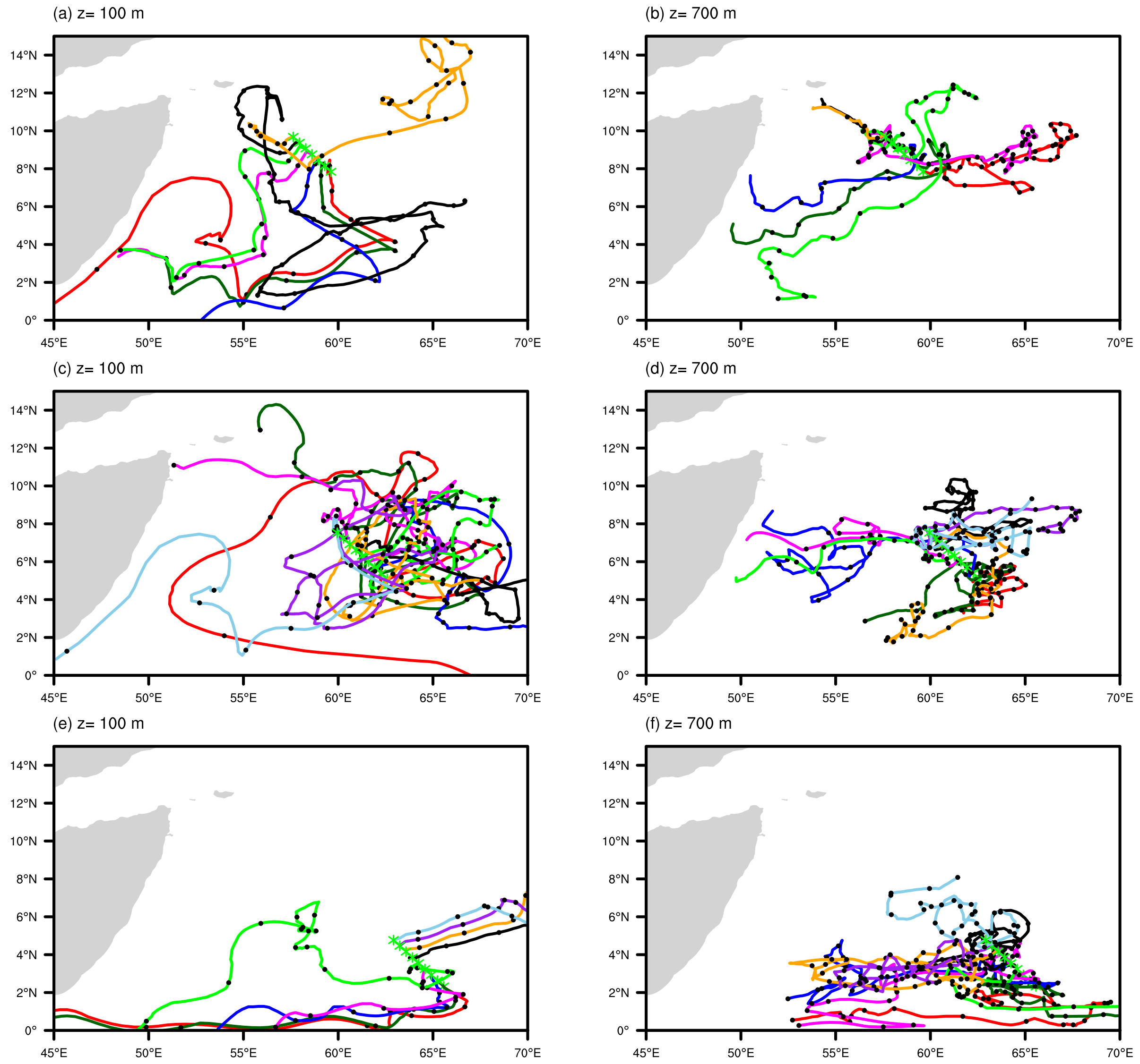

Figure 6. Passive tracers using SODA reanalysis. ~~The tracers are set along the CR on May 15, 2012 (denoted by green asterisks), and then backward integrated to Jan. 1, 2010.~~ The time interval is one month, as denoted by the black dots. (a-b) 8-9.8°N; (c-d) 5-8°N; (e-f) 2-5°N.